Accuracy of down-facing surfaces in complex internal channels produced by laser powder bed fusion (L-PBF)

Available online at www.sciencedirect.com

ScienceDirect

Procedia CIRP 88 (2020) 423–426

www.elsevier.com/locate/procedia

13th CIRP Conference on Intelligent Computation in Manufacturing Engineering, CIRP ICME '19

# Accuracy of down-facing surfaces in complex internal channels produced by laser powder bed fusion (L-PBF)

Flaviana Calignano[a,*], Luca Iuliano[a], Manuela Galati[a], Paolo Minetola[a], Giovanni Marchiandi[a]

[a]*Dipartimento di Ingegneria Gestionale e della Produzione, Politecnico di Torino, Corso Duca degli Abruzzi, 24, Turin, Italy*

* Corresponding author. Tel.: +0-011-090-7218; fax: +0-011-090-7299. E-mail address: flaviana.calignano@polito.it

**Abstract**

Additive manufacturing (AM) technology has great potential in manufacturing complex internal channels for several applications such as satellite communication systems, electronics and gas turbine airfoils. These applications can have complex shape and make traditional finishing processes a challenge for additive parts. Therefore, it is desirable that the internal surfaces be as close as possible to the tolerance of the field of application. In this study, a complex component was designed and manufactured in AlSi10Mg alloy through laser powder bed fusion (L-PBF) process. Using the data from the 3D scans, internal surface roughness and deviations from the CAD model were calculated.


Peer review under the responsibility of the scientific committee of the 13th CIRP Conference on Intelligent Computation in Manufacturing Engineering, 17-19 July 2019, Gulf of Naples, Italy.

*Keywords:* Additive Manufacturing; Selective Laser Melting; Laser Powder Bed Fusion; Internal Channels; Accuracy; Surface Roughness

## 1. Introduction

Laser powder bed fusion (L-PBF) is an additive manufacturing (AM) process, where layers of metal powder are sequentially fused by a high-power laser. L-PBF has the potential for manufacturing complex internal channels for several applications such as satellite communication systems, electronics and gas turbine airfoils. However, the surface texture, growing in a bed of powder, is affected by a number of factors, including the particle size distribution of the powder, the effect of the thermal conductivity, the layer thickness, the angle of the surface relative to the horizontal build bed and the effect of any post-processing/finishing. Each layer is created by melting selected areas of a layer of powder, which consolidates and merges with the layer below. Certain conditions in the melt pool can induce 'balling' of the molten material, which can then disrupt the edge of the melt pool, affecting the shape of the layer edge. Gravity also affects the melting well for layers that are not supported and that collapse into the un-melted powder below, resulting in a much rougher surface on the underside of the component (called 'down-skin') than on the upward facing surfaces (called 'up-skin'). This difference between two surfaces is compounded by the unequal heat dissipation rates in powder, compared to the solid material, which create thermal gradients and destabilizes the melt pool, further disrupting the shape of the layer edge [1]. When the melt pool solidifies, partially melted particles from the surrounding powder also adhere to the edge of the layer and this also contributes to the final surface structure.

L-PBF requires the use of additional structures to support the weight of protruding geometries when the amount of overhang exceeds a certain value, attaching the component to the platform and helping to dissipate heat [2]. However, these structures cannot be inserted inside channels because it would be difficult and in some cases impossible to remove them. Although therefore, self-sufficient internal channels are built, there is still the formation of dross on the down-skin surface. The L-PBF machine software allows to assign different construction parameters for up-skins, down-skins and cores.

In this study, a complex radio frequency (RF) component, designed for integral integration into a single waveguide component three features, namely filtering, bending and torsion [3], manufactured in AlSi10Mg alloy by L-PBF, was analyzed using 3D scan data. The down-skin and up-skin zones were compared in terms of surface roughness and geometric deviations from the CAD model.


Peer review under the responsibility of the scientific committee of the 13th CIRP Conference on Intelligent Computation in Manufacturing Engineering, 17-19 July 2019, Gulf of Naples, Italy.
10.1016/j.procir.2020.05.073

## 2. Case study

A monolithic waveguide system, named WR51 and operating in Ku/K-bands, was design in order to reduce mass and miniaturize a dual-band dual-polarization waveguide antenna-feed chains through AM (Figure 1) [3].

The configuration of the integrated component shown in Figure 1b can hardly be produced by conventional processes such as milling, turning, or processing of electric discharges. More complex technologies, such as electroforming, can be applied in order to construct a single-block component, but some problems, such as the necessary equipment and the rigidity of the material, must be carefully considered. Therefore, the design of this component was carried out starting from the choice of additive technology, in particular the L-PBF process, as it allows the development of very high density monolithic metal components (> 99.5% compared to bulk material), good mechanical properties, such as tensile strength and hardness [4-7], and a much lower surface roughness than that obtainable by another PBF process, namely the electron beam melting (EBM). Before the construction of the integrated component, the configurations designed were subjected to statistical sensitivity analysis in order to evaluate the robustness of the component with respect of the L-PBF process. In this way, it was possible to evaluate the applicability of the internal conformation of the proposed channel with respect to various technological problems, such as removal of the powder from the internal channels.

The CAD model has been converted into a STL file whose setting, such as deviation control and angle, have been chosen to define a STL-model that is fairly smooth and accurate so as to ensure negligible discrepancies between the electromagnetics responses of the STL and 3D CAD models. The internal edges of the component are rounded to 0.1 mm to avoid geometric errors due to the size of the laser diameter based on the process parameters used. It has been verified that this rounding does not substantially affect the RF performance of the component. The orientation of the component on the platform is chosen to make the internal channel self-supporting (Figure 2). The supports were inserted only externally to anchor the part to the building platform.

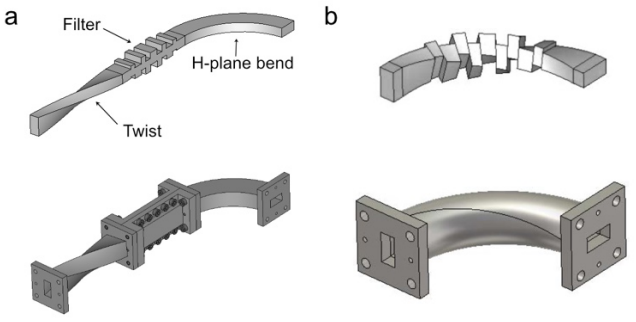


Fig. 1. (a) Internal structure and mechanical assembly of a reference WR51 waveguide subsystem consisting of an H-plane 90° bend, a 90° twist, and a low-pass filter; (b) WR51 waveguide component integrating bending, twisting, and filtering functionalities with the same scale factor.

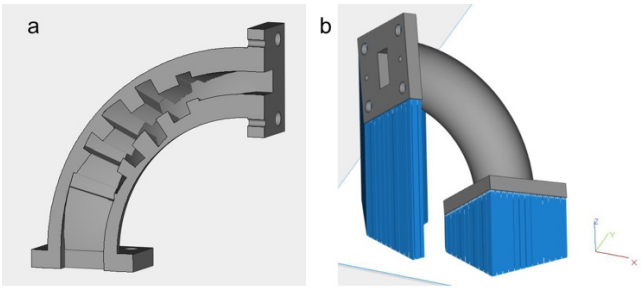


Fig. 2. (a) CAD model; (b) orientation of the component on the building platform.

## 3. Equipment

The AlSi10Mg filters have been built through an EOSINT M270 Dual-mode system equipped with an 200W Yb-fiber laser and a beam-spot size of 100 μm. The manufacturing process is carried out within a chamber filled with inert gas (argon), ensuring an oxygen content lower than 0.10 %. The main L-PBF system parameters used are shown in Table 1 [8]. As scanning strategy, the direction of scanning is rotated of 67° between consecutive layers. Correct optimization of process parameters (i.e., beam offset and scanning options) allows dimensional accuracy to be achieved within 0.04 and 0.07 mm, and an equivalent surface electrical resistivity of approx. 10-20 μΩ are feasible for this alloy. The building platform is heated at 100°C to reduce thermal stresses that arise during the process. A layer thickness of 30 μm was chosen.

Table 1. Process parameters

| Process parameters | Core | Down-skin (3 layers) | Up-skin (2 layers) | Contour |
|---|---|---|---|---|
| Laser power [W] | 195 | 190 | 190 | 80 |
| Scan speed [mm/s] | 800 | 900 | 800 | 900 |
| Hatching distance [mm] | 0.17 | 0.10 | 0.10 | |

The component was sectioned in order to investigate the surface roughness and accuracy between the two different zones, the lower one in which the inner zone corresponds mostly to the up-skin and the upper area in which the part internal corresponds to the down-skin. The two part of the prototype were digitized by means a 3D optical scanner, Atos Compact Scan 2M by GOM GmbH, and GOM Inspect software was used for the inspection. Detailed images of some internal surfaces were provided by a Leica S9i stereomicroscope. The surface roughness of sample was measured with the use of RTP80 roughness tester by SM Metrology Systems.

## 4. Result and discussion

In order to assess the absence of defects and to inspect the surface quality, the prototype has been cut in the H-plane of the right-hand input rectangular waveguide port. The result of deviation analysis between the 3D CAD model and the model produced by L-PBF process is shown in Figure 3.

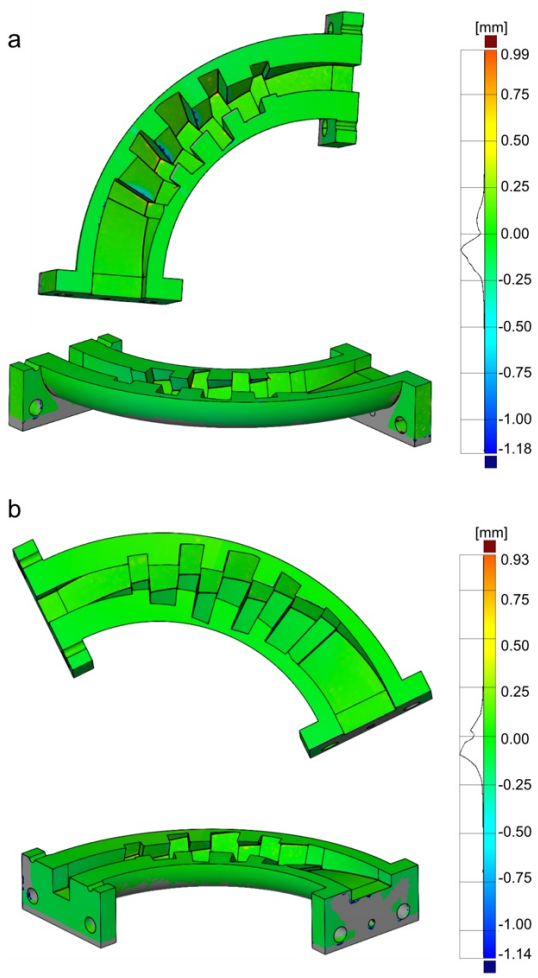


Fig. 3. Color map of the deviation analysis for the (a) down-skin and (b) up-skin surfaces

The internal down-skin (Figure 3a) and up-skin (Figure 3b) areas both have an average deviation of about 0.08 mm from the CAD model. From Figure 4 it can see that the deviation is on some edges of the overhanging areas. This deviation is not due to the so-called staircase effect, typical of additive technologies, but by the dross formation. Staircase effect is a phenomenon happening during the fabrication of overhanging structures. The overhanging length $L_o$ between adjacent two layers can be determined as follow [9]:

$$L_o = \frac{t}{tan\theta} \quad (1)$$

Where $t$ is the layer thickness and $\theta$ is the inclined angle defined as the angle between the horizontal plane and the tangent line of the surface. From Eq. (1) it can easily be deduced that a decrease of the inclined angle $\theta$ can lead to a larger protruding length $L_o$ and therefore give rise to a prominent staircase effect, which negatively affects the quality of the overhanging structures. Therefore, it is evident that the use of a thin powder layer in the L-PBF process avoids the occurrence of the staircase effect. A thin layer of 30 μm was used for the construction of the component.

Dross formation is considered the most unpredictable and difficult to control manufacturing defect of the L-PBF process.

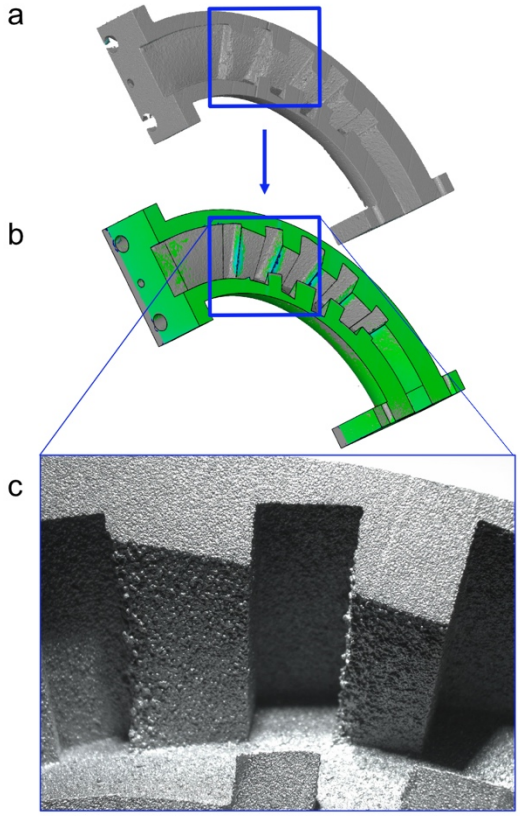


Fig. 4. Down-skin surface as oriented on the building platform:(a) production prototype; (b) color map of the deviation analysis; (c) stereomicroscope image

This defect involves a great surface roughness and a poor geometrical precision of the overhanging surfaces. Analyzing the process parameters used, three different energy density $E$ [10] of 70 J/mm$^3$, 79 J/mm$^3$ and 47.79 J/mm$^3$ were used for down-skin, up-skin and core respectively. According to some studies [11,12], the formation of a small melt pool can reduce the occurrence of dross formation and improve the down-skin surface fabrication quality significantly. However, the use of a low $E$ (about 48 J/mm$^3$) can effectively reduce the size of the melt pool but give rise to the partial fusion of the manufactured part causing an unfavorable bonding between the neighboring melting tracks, a detrimental effect for the manufacturing success of full-density L-PBF overhanging part. If the problem is tackled based on the value of the energy of density, to solve the defects due to the dross formation, it would be enough to remain in a range of 60 – 80 J/mm$^3$ [11]. However, the case study showed that the use of an energy value of 70 J/mm$^3$ also leads to the dross formation. This is because the energy value depends on the numerical combination of the parameters. The same value can be obtained with different process parameters leading to different results [10, 13, 14]. Surely, the formation of dross and spatter is due to the high laser absorptivity of the powder compared to the solid metal in the bulk of the part. Furthermore, the presence of these dross only in the edges shows that the problem can be caused by an incorrect choice of rounding the edge, or by the combination of the process parameters between the contour and down-skin or both. In fact, the inclination of these area gradually increases as the

component grows in height, exceeding 45 degree of slope. Despite this, the edge suffered the greatest defect. The edge can be considered a small feature of a model. For features with dimensions comparable to the hatching distance, the actual location of the model contour could significantly affect the hatch line generation, which potentially results in both dimensional and positional error for the final shape [15].

The surface roughness measured on the down-and up-skin faces is about 8 μm ± 1.3 μm ($R_a$, arithmetic mean of the profile deviation from the average measured line) that it is lower than that normally obtained with AlSi10Mg alloy for this technology (10-20 μm).

## 5 Conclusion

The results obtained on the dimensional accuracy of a complex component for RF showed the potential prospective capability of L-PBF process in the miniaturization of waveguide components for terrestrial and space communications. Accuracy and surface quality provided by L-PBF is already suitable for monolithic production of waveguide components. However, there are still inherent problems with technology that are currently only reduced but not eliminated.

## Acknowledgements

The Authors thank Dr. Peverini O.A. and Dr. Addamo G. of the CNR-IEIIT Institute for their constant trust and collaboration in the application of additive manufacturing technologies in the field of RF.

## References

[1] Vandenbroucke B, Kruth J-P. Selective laser melting of biocompatible metals for rapid manufacturing of medical parts. Rapid Prototyping J.2007; 13196–203

[2] Calignano F. Design optimization of supports for overhanging structures in aluminum and titanium alloys by selective laser melting. Materials & Design, 2014; 64: 203-213

[3] Peverini O, Lumia M, Addamo G, Paonessa F, Virone G, Tascone R, Calignano F, Cattano G, Manfredi D. Integration of an H-plane bend, a twist, and a filter in Ku/K-band through additive manufacturing. IEEE Transactions on Microwave Theory and Techniques (2018), 66: pp.2210-2219.

[4] Trevisan F, Calignano F, Lorusso M, Pakkanen J, Aversa A, Ambrosio E.P., Lombardi M, Fino P, Manfredi D. On the selective laser melting (SLM) of the AlSi10Mg aaloy: process, microstructure, and mechanical properties. Materilas, 2017; 10(1): 76

[5] Shifeng W, Shuai L, Qingsong W, Yan C, Sheng Z, Yusheng S. Effect of molten pool boundaries on the mechanical properties of selective laser melting parts. J. Mater. Process. Technol. 2014;214:2660–2667.

[6] Lu Y, Wu S, Gan Y, Huang T, Yang C, Junjie L, Lin J. Study on the microstructure, mechanical property and residual stress of SLM inconel-718 alloy manufactured by differeing island scanning strategy. Opt. Laser Technol. 2015;75:197–206

[7] Brandl E, Heckenberger U, Holzinger V, Buchbinder D. Additive manufactured AlSi10Mg samples using Selective Laser Melting (SLM): Microstructure, high cycle fatigue, and fracture behavior. Mater. Des. 2012;34:159–169

[8] Calignano F, Manfredi D, Ambrosio EP, Iuliano L, Fino P. Influence of process parameters on surface roughness of aluminum parts produced by DMLS. Int. J. Adv. Manuf. Technol. 2013; 67: 2743-2751

[9] Yadroitsev I, Thivillon L, Bertrand P.h., Smurov I. Strategy of manufacturing components with designed internal structure by selective laser melting of metallic powder. Appl. Surf. Sci. 2007; 254: 980–983.

[10] Scipioni Bertoli U, Wolfer AJ, Matthews MJ, Delplanque JPR, Schoenung JM On the limitations of volumetric energy density as a design parameter for selective laser melting. Mater. Des. 2017; 113: 331–340.

[11] Chen H, Gu D, Xiong J, Xia M. Improving additive manufacturing processability of hard-to-process overhanging structure by selective laser melting. Journal of Materials Processing Tech. 2017; 250: 99-108

[12] Charles A, Elkaseer A, Thijs L, Hagenmeyer V, Scholz S. Effect of process parameters on the generated surface roughness of down-facing surfaces in selective laser melting. Appl. Sci. 2019; 9: 1256

[13] Prashanth KG, Scudino S, Maity T, Das J, Eckert J. Is the energy density a reliable parameter for materials synthesis by selective laser melting? Mater. Res. Lett., 2017; 1–5.

[14] Calignano F, Cattano G, Manfredi D. Manufacturing of thin wall structures in AlSi10Mg alloy by laser powder bed fusion through process parameters. Journal of Materials Processing Tech., 2018; 255: 773-783.

[15] Yang L, Gong H, Dilip S, Stucker B. An investigation of thin feature generation in direct metal laser sintering systems. Solid Freeform Fabrication Symposium, The University of Texas at Austin, August 4-6, 2014; 714-731